

Inclined dislocation-pair relaxation mechanism in homoepitaxial green GaInN/GaN light-emitting diodes

Mingwei Zhu (朱明伟),¹ Shi You (尤适),¹ Theeradetch Detchprohm,¹ Tanya Paskova,² Edward A. Preble,² Drew Hanser,^{2,*} and Christian Wetzel¹

¹*Future Chips Constellation, and Department of Physics, Applied Physics, and Astronomy, Rensselaer Polytechnic Institute, 110 Eighth Street, Troy, New York 12180, USA*

²*Kyma Technologies, Inc., 8829 Midway West Road, Raleigh, North Carolina 27617, USA*

(Received 2 September 2009; revised manuscript received 29 January 2010; published 22 March 2010)

The creation of symmetrical pairs of inclined dislocations was observed in the GaInN/GaN quantum wells (QWs) of *c*-axis grown green light-emitting diodes (LEDs) on low-defect density bulk GaN substrate, but not in green LEDs on sapphire substrate with high threading dislocation (TD) density. Pairs of dislocations start within 20 nm of the same QW and incline 18° – 23° toward two opposite $\langle 1\bar{1}00 \rangle$ directions or in a 120° pattern. We propose that in the absence of TDs, partial strain relaxation of the QWs drives the defect formation by removal of lattice points between the two dislocation cores. In spite of those inclined dislocation pairs, the light output power of such green LEDs on GaN is about 25% higher than in LEDs of similar wavelength on sapphire.

DOI: [10.1103/PhysRevB.81.125325](https://doi.org/10.1103/PhysRevB.81.125325)

PACS number(s): 61.72.Ff, 78.67.De, 81.05.Ea

I. INTRODUCTION

High efficiency blue light-emitting diodes (LEDs) have been achieved with GaInN/GaN heterostructures in the active region.¹ Such structures also hold the highest promise for the green and deep green spectral regions when a higher InN fraction in the GaInN quantum wells (QWs) can be achieved.^{2,3} This requires management of higher strain within this highly lattice mismatched system and its propensity of defect generation, such as misfit dislocations (MDs) (Refs. 4 and 5) and V defects.^{6,7} In heteroepitaxy on sapphire substrate, typically a high density of threading dislocations (TDs), emanating from the heterointerface with the substrate, propagates into the active region.¹ Our earlier work has shown that the performance of green LEDs strongly scales with the suppression of such defects in the active region.^{3,8} With recent advances in hydride vapor-phase epitaxy (HVPE) and surface preparation, bulk GaN wafers⁹ with TD densities as low as $<5 \times 10^6 \text{ cm}^{-2}$ should therefore prove an ideal substrate for homoepitaxial growth.

Here we study the microstructural properties of green GaInN/GaN LEDs grown on such low-dislocation density bulk GaN. In the absence of TDs we find a new type of defect that—without a precursor dislocation—appears in pairs and inclines from the growth direction. We analyze the range of known microscopic dislocation forces and find a good description in the Peach-Koehler force¹⁰ resulting from a macroscopic relaxation of strain.

II. CRYSTAL GROWTH

c plane bulk GaN substrate of size $(1 \text{ cm})^2$ was obtained by HVPE and prepared for homoepitaxy by chemomechanical polishing of the Ga-face surface to an atomic level of flatness. The surface roughness as measured by atomic force microscopy over a $(5 \text{ }\mu\text{m})^2$ area was 0.1–0.2 nm (root mean square). Homoepitaxy of the full LED structures¹¹ was performed by metalorganic vapor-phase epitaxy. The typical de-

vice structure consists of 0.5- μm -thick epitaxial *n*-type GaN, ten periods of GaInN/GaN QWs, a 15-nm-thick *p*-type Al-GaN electron blocking layer, and 180-nm-thick *p*-type GaN. The nominal thicknesses of QWs and barriers are 3 nm and 20 nm, respectively. For comparison, two structures (samples A and B) were grown on bulk GaN, and the same structure was grown on 4- μm -thick *n*-GaN template on *c*-plane sapphire (sample C). Electroluminescence was evaluated by using 1 mm diameter indium contacts on the scratched wafer surface. In our experiment such results are a reliable indicator for fabricated LED performance. The dominant wavelengths were observed at 532 nm (sample A) and 537 nm (samples B and C) at a current density of 2.5 A/cm^2 . Samples discussed here were grown over a period of seven months and the results discussed here are deemed characteristic for the trends seen. The $\text{Ga}_{1-x}\text{In}_x\text{N}$ alloy fraction *x* was determined by combining x-ray diffraction data of the averaged GaInN/GaN layers and the GaN substrate with the actual well thickness as determined by transmission electron microscopy (TEM). Using a standard model of elastic strain deformation we find $x \approx 10\%$. We are aware, that other groups quote higher numbers to reach the same wavelength range.¹² Portions of the samples were analyzed in TEM at 120 kV (Philips CM12) and 200 kV (JEOL 2010). Both, cross-sectional and plan-view samples were prepared by mechanical polishing, followed by ion milling at 3–5 kV (Fischione 1010).

III. PROPERTIES OF INCLINED DISLOCATION PAIRS

The cross-sectional TEM of the green LED on bulk GaN (sample A) reveals the layers of *n*-GaN, multiple QWs (MQWs), *p*-AlGaN, and *p*-GaN [Fig. 1(a)]. Throughout the observable sample width of 10 μm , we cannot find any TDs generated in the homoepitaxial interface nor propagating from the bulk substrate. This is consistent with the low TD density of the bulk substrate identified at $<5 \times 10^6 \text{ cm}^{-2}$,

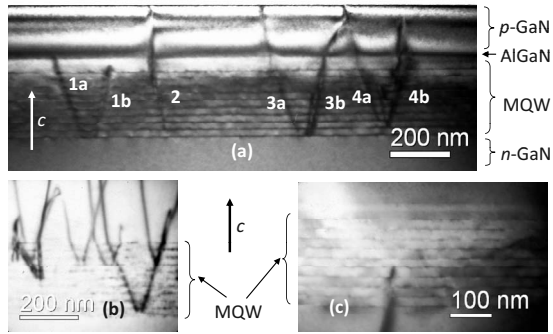


FIG. 1. TEM images of green LED samples on bulk GaN substrates [(a) sample A, recorded along $[1\bar{2}\bar{1}0]$; (b) sample B, near $[1\bar{1}00]$ zone axis] and on sapphire substrate [(c) sample C, along $[1\bar{2}\bar{1}0]$]. Inclined dislocation pairs can be seen in the samples A and B on GaN, but not in sample C on sapphire.

proving our epitaxial capability to replicate its quality in homoepitaxy. However, MDs appear to be generated in the active region of the sample. Most of them start within the first three QWs without any observable precursor defect. Instead of propagating along the growth direction (c axis) as typical for TDs, all MDs are inclined at some angle off the $[0001]$ c axis. Most come in pairs to form inclined dislocation pairs (IDPs). The dislocations of one pair are found to start together in the same QW within a short separation (~ 20 nm) and branch off to different sides of the $[0001]$ direction. For example, dislocations 1a and 1b, 3a and 3b, 4a and 4b form three IDPs [Fig. 1(a)]. Dislocation 2 appears as a sole branch. It is likely that its pairing branch extended out of the plane and was removed during the thinning process. We estimate a dislocation density of $6 \times 10^9 \text{ cm}^{-2}$, yet do not find any formation of V defects. In the second green LED on bulk GaN (sample B), generation of IDPs is seen throughout all QWs [Fig. 1(b)].

The inclination of individual dislocations has been observed in c axis grown GaN and AlGaIn layers before.^{13–19} For example, a bending of dislocations could be induced in GaN by beryllium¹³ or oxygen¹⁴ doping. Inclination of dislocations was also observed when threading from high AlN-fraction AlGaIn to layers of lower AlN fraction^{15,16} and later explained by Romanov and Speck¹⁷ with a strain release mechanism involving an “effective climb.” In this model, adatoms experience directional diffusion along the growth surface toward pre-existing TDs where they incorporate. They also calculated conditions, under which the operation of this mechanism is energetically favored. Follstaedt *et al.*¹⁸ argued that the bending could occur by jogs of the dislocation line. In his process, growth terraces overgrow the vacancies left by dislocation cores. Besides those premeditated by individual TDs propagating along the c axis, generation of inclined dislocation was observed in tensile strained AlN/GaN QWs.¹⁹ Throughout the GaInN system, however, to our understanding there are no reports of inclined dislocations in the literature. The lattice mismatch between InN and GaN is very different from that of AlN and GaN and due to the softer bonds, the formation energy of defects should be much lower, too. So the case of inclined dislocations in GaInN layers definitely warrants study.

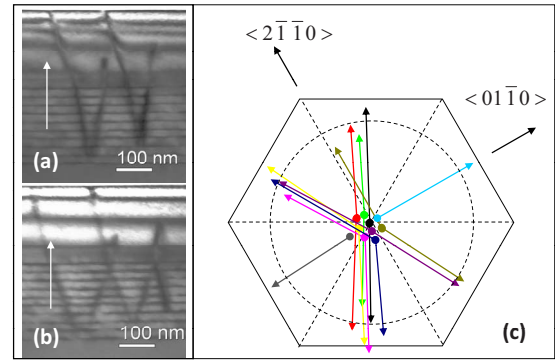


FIG. 2. (Color online) TEM images of IDPs recorded along (a) the $[11\bar{2}0]$ zone axes; (b) the $[1\bar{2}\bar{1}0]$ zone axes. (c) A schematic illustration of the projections of inclined dislocations and IDPs in top view of the sample. The dislocations predominantly point in the $\langle 1\bar{1}00 \rangle$ directions, inclined by 18° – 23° from the $[0001]$ direction (white arrows).

For the green LEDs on sapphire [e.g., sample C, Fig. 1(c)], we only find very few dislocations to be generated within the active region. Instead, most dislocations propagate from the n -GaN template underneath. Unlike frequent reports in the literature,^{6,7} no V defects were generated as these dislocations penetrate the active MQW region in these optimized structures. All of the dislocations propagate along the $[0001]$ direction and do not lead to the formation of IDPs nor individual inclined dislocations. The same holds for other GaInN-based blue or green LED structures on sapphire studied by this group. We find that IDPs are unique to the homoepitaxial green LEDs on low-dislocation density bulk GaN substrate. In contrast to this case of inclined dislocations, horizontal MDs along $\langle 1\bar{1}00 \rangle$ directions have been reported in thick GaInN films by Srinivasan *et al.*²⁰ and Liu *et al.*²¹ Similar to our case, such observation was limited to films on low-defect-density ($< 10^7 \text{ cm}^{-2}$) GaN templates and could not be seen in samples simultaneously grown on GaN on sapphire templates with high TD density ($\sim 10^9 \text{ cm}^{-2}$).²⁰

By rotating the sample under TEM, the propagation directions of the inclined dislocations were determined. Figure 2 shows two IDPs recorded along the zone axes $[11\bar{2}0]$ [Fig. 2(a)] and $[1\bar{2}\bar{1}0]$ [Fig. 2(b)]. Since some dislocations disappear or change direction in the p layers, we limit this analysis to the MQW region. The propagation direction of dislocations was determined from their apparent angle with the $[0001]$ c axis in both projections. The results are summarized in a top view illustration [Fig. 2(c)], where the dislocations are represented by a basal plane projection of their unit length vector (for clarity, vectors are arranged around the origin of a hexagonal cell). Dislocations of a pair share color and starting point. Most of the dislocations are inclined toward either of the $\langle 1\bar{1}00 \rangle$ m directions at an angle of 18° – 23° . Such angles are within the range observed in AlGaIn as premeditated by vertical dislocations in GaN.¹⁵ Dislocations of one pair branch off in opposing directions, either at a 180° or a 120° separation. Apparently, all inclined dislocations and IDPs are orientated with a high degree of symmetry.

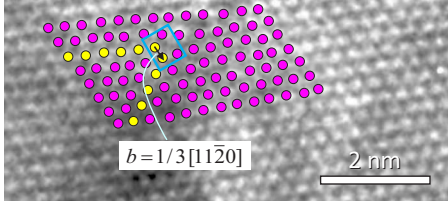


FIG. 3. (Color online) High-resolution plan-view TEM image of LED on GaN (sample A). The colored dots correspond to the Ga column sites around a dislocation. The core of an edge-type dislocation with Burgers vector $1/3[11\bar{2}0]$ is illustrated in the blue rectangle. The dislocation can be viewed as the intersection of two half $\{1\bar{1}00\}$ planes (yellow dots).

A plan-view high-resolution TEM image of the top p -GaN of the LED on bulk GaN (sample A) reveals the dislocation core (Fig. 3). Ga atom sites around the core are labeled by colored dots. The four atoms in the blue rectangle correspond to the Ga atoms in the eightfold ring dislocation core, similar to those observed by Xin *et al.*²² The dislocation can be described by the intersection of two extra $\{1\bar{1}00\}$ half planes of atoms (yellow dots). A Burgers circuit around the dislocation reveals a displacement component of $1/3[11\bar{2}0]$. When the sample is tilted to $\mathbf{g}=[0002]$, the dislocations fall out of contrast revealing their pure edge-type nature with Burgers vector $\mathbf{b}=1/3\langle 11\bar{2}0 \rangle$. These vectors are perpendicular to the c -plane projection of dislocation lines, as determined from plan-view TEM.

IV. DISCUSSION

Both cores are expected to interact by a range of forces. With opposite Burgers vectors, their strain fields provide an attractive force²³ $F_i = \frac{Gb^2h}{2\pi(1-\nu)} \frac{1}{r}$, (bulk modulus²⁴ $G = 196$ GPa, Burgers vector \mathbf{b} , and Poisson ratio²⁴ $\nu = 0.21$) and at $r = 20$ nm separation, the force should be $|F_i| = 0.6$ nN over the $h = 3$ -nm-thick GaInN layer. On the other hand, the misfit force²⁵ can be written as $F_m = 2Gb\varepsilon \frac{1+\nu}{1-\nu} h \cos \lambda$, where ε is lattice mismatch strain and λ is the angle between Burgers vector and the direction on the interfacial plane perpendicular to the dislocation line. It amounts to a force $|F_m| = 5.7$ nN, along the Burgers vector, i.e., perpendicular to the observed dislocation separation. Next, line tension²⁵ $F_l = \frac{Gb^2}{4\pi} \frac{1-\nu \cos \alpha}{1-\nu} [\ln(\frac{h}{b}) + 1]$ (angle α between misfit dislocation line and Burgers vector) is a resistive force and prevents a dislocation from moving or bending. It here amounts to $|F_l| = 6.5$ nN. Negligible on that scale is the Peierls force²⁶ with $|F_p| < 10^{-3}$ nN. If we compare forces accumulated over the GaInN layer, line tension is the largest, while the apparent mechanism separating the dislocations is climbing. Therefore, an expression for a climb force reflecting our observations needs to be found.

In Romanov's energy balance model,¹⁷ for a given strain condition, the energy change depends on the film thickness and dislocation inclination angle. The most likely inclination is expected for small inclination angles in thicker films. According to this model, our observation of the generation of a

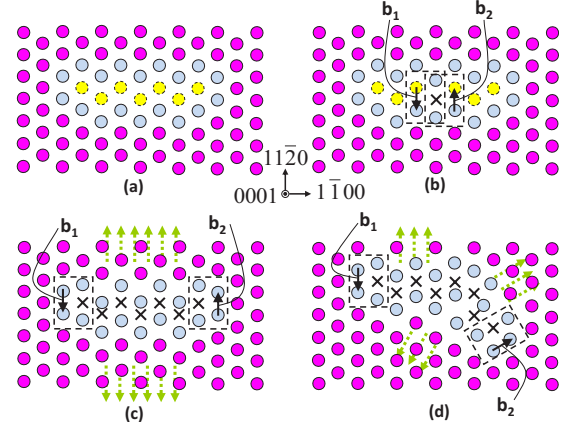


FIG. 4. (Color online) Illustration of the atom array in c planes before (a), during (b) and after (c) the formation of an IDP in 180° configuration. Dashed dots mark the sites of atoms to be removed, leaving an \times mark behind. Blue dots represent their nearest neighbors. Dashed rectangles show the dislocation cores and their Burgers vectors (arrows). Starting with one atom (b), two dislocation cores move apart while releasing compressive strain between them (green arrows indicate directions of relaxation). (d) The same process schematically shown in 120° configuration.

single straight dislocation in a 3-nm-thick GaInN QW (10% InN fraction, 1.1% strain) should cost a formation energy of $\sim 6Gb^3$ and its inclination by 20° should add $\sim 0.8Gb^3$. Accordingly, an inclination should not be energetically favored. Therefore, their model seems not satisfactory to predict dislocation inclination in the GaInN material system.

The occurrence of IDPs only in highly strained green emitting layers on low-TD density GaN templates leads us to speculate that their generation provides a mechanism of partial strain relief. We therefore develop a model of partial relaxation of biaxial strain. We consider dislocation climb at the growth front, which is far more likely than bulk climb.^{16,17} A sequence of progressive layer growth of the Ga or In sublattices is schematically shown in Figs. 4(a)–4(c). Possible intermediary layers are omitted. As the overall driving force for the generation of IDPs, we consider the relaxation of biaxial compressive strain in the pseudomorphic GaInN layer on the relatively strain-free GaN substrate. For this, we progressively remove a line of atoms [yellow dashed dots in Fig. 4(a)]. At the initiation point, a first atom is not incorporated into the layer, leaving a hollow center (“ \times ” mark) between six neighboring atoms [Fig. 4(b)]. Any four neighboring atoms in the hexagon can be seen as the core of an edge-type dislocation, as observed in TEM (Fig. 3). The two dislocation cores move apart as more atoms are removed between them. Every removed atom provides a strain relief parallel to the Burgers vector. By sequential separation of the cores along either of the $\langle 1\bar{1}00 \rangle$ directions with every new grown layer, a longer line of atoms is removed and a larger fraction of the growth plane can be relaxed. The divergence of the dislocations is largest when they are separated by 180° [Fig. 4(c)] and somewhat smaller when separated by 120° [Fig. 4(d)].²⁷ A separation of 60° only produces a very slow separation. This can well explain our findings that IDPs separate at either 180° or 120° .

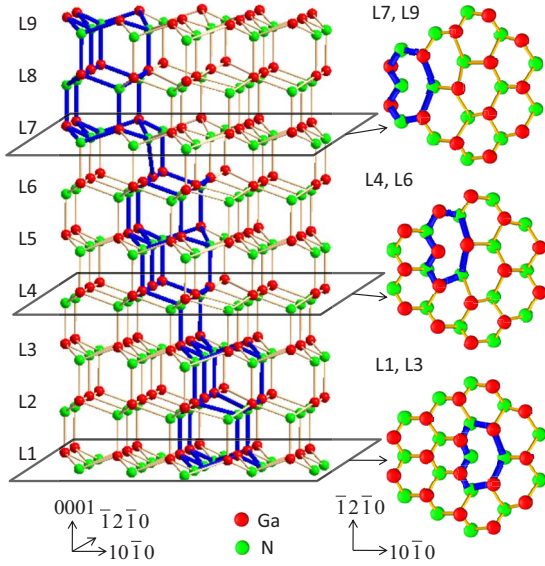


FIG. 5. (Color online) Illustration of an inclined dislocation in the three-dimensional lattice. The dislocation jumps by one lattice constant $1/3[\bar{1}\bar{1}20]$ or $1/3[\bar{2}110]$ every three layers during $[0001]$ growth. These cumulative movements lead to a dislocation inclination toward $[\bar{1}010]$ direction by 20° .

The inclination of one branch of an IDP in the crystal lattice is schematically shown in Fig. 5. Atomic layers are denoted from L1 through L9, where L7 is an offset repetition of L1. The bonds of the dislocation core are highlighted in thick blue lines. Within the growth plane, they form an eight-fold ring. In three dimensions, it forms a slanted tube. During $[0001]$ lattice growth, the dislocation core alternatively jumps by basal plane vectors $1/3[\bar{1}\bar{1}20]$ or $1/3[\bar{2}110]$ every three atomic layers. This sequence of core movements leads to a dislocation inclination to $[\bar{1}010]$ directions by an angle of 20° . This independently developed model of alternate basal plane jumps differs from that by Follstaedt *et al.*¹⁸ of a direct $[\bar{1}010]$ jump by the additional intermediary step that should result in a lower total cost of strain energy. The in-plane layouts of Ga and N atoms are also shown for layer pairs (L1, L3), (L4, L6), and (L7, L9) of the three-layer groups. The other layers are mirror reflections of the preceding layers with a Ga-N-atom exchange. For clarity, necessary lattice relaxation around the described cores is omitted in the figure. With every additional layer the dislocation climbs to the left and fewer atoms are incorporated indicating the relaxation of the GaInN film.

A microscopic climb force F_c can be determined from the released compressive strain energy in the newly relaxed area when an additional atom remains unincorporated. The energy density of the strained layer is calculated²⁸ as $(c_{11} + c_{12} - 2\frac{c_{13}^2}{c_{33}})\epsilon^2$ with strain ϵ and the elastic stiffness constant c_{ij} from interpolating between GaN and InN by assuming the validity of Vegard's law.²⁴ We assume that the displacement of the missing atoms is uniformly spread to $N=1/\epsilon$ lattice points in directions parallel to the Burgers vectors of the IDPs. The effective climb force can then be written as

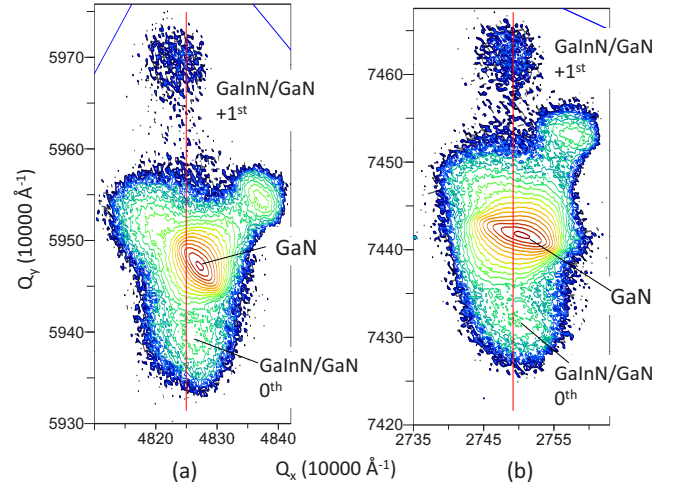


FIG. 6. (Color online) Reciprocal space mapping around the (a) $(11\bar{2}4)$ and (b) $(10\bar{1}5)$. X-ray diffraction maxima of GaN in the green LED on bulk GaN (sample A). The GaInN/GaN MQW peaks are offset from the GaN peaks by $\sim 0.06\%$ along the reciprocal x axis for both mappings, corresponding to a relaxation of $\sim 5\%$.

$$F_c = \frac{1}{2} a_{\text{GaInN}} h \left(c_{11} + c_{12} - \frac{2c_{13}^2}{c_{33}} \right) \epsilon, \quad (1)$$

where a_{GaInN} is the in-plane lattice constant of fully relaxed GaInN. This expression is equivalent to the Peach-Koehler force¹⁰ $F = P \times \tau$, with $P_i = \sum \sigma_{ij} b_j$ (stress tensor σ_{ij} , Burgers vector b_j) and τ is the unit tangent vector to the dislocation line. The difference is a factor 1/2 in our model which accounts for the uniaxial relaxation along the Burgers vector.

For a typical $h=3$ nm QW with 10% InN fraction, the strain is $\epsilon=1.1\%$, resulting in $F_c=2.1$ nN. The climb force is of similar magnitude as those considered above, yet it is smaller than the line tension.

The observation of dislocation climb apparently cannot satisfactorily be predicted using the detailed force analysis of individual dislocations. We therefore resort to a more macroscopic description of strain relaxation.

By reciprocal space mapping in x-ray diffraction, we analyze the degree of GaInN lattice relaxation in sample A on bulk GaN in reference to the GaN host lattice. The GaN barrier should be strained to the GaInN QW underneath. Along the $(11\bar{2}4)$ diffraction, the a lattice constant is monitored along the x axis [Fig. 6(a)], while in $(10\bar{1}5)$ diffraction, the x axis corresponds to the m axis in the lattice [Fig. 6(b)]. The GaInN/GaN QW satellite peaks reveal maxima offset by -0.06% in reciprocal a axis and -0.06% in reciprocal m axis. This corresponds to a 5% biaxial strain relaxation of the averaged GaInN/GaN MQW in reference to the pseudomorphic strain condition. To correlate this average strain relaxation $\Delta\epsilon$ of the strain ϵ in the QWs with the dislocations as observed, we consider the case for 180° IDPs. With an average separation \bar{r} of two dislocation cores in the QW, the area relaxed in one dimension by each IDP is $1/2 \bar{r} N a_{\text{GaInN}}$. With an IDP area density of ρ , the fraction of relaxation then is given by

$$\overline{\Delta\epsilon} = \frac{A_{relaxed}}{A_{total}} = \frac{1}{2} \rho \bar{r} N a_{\text{GaInN}}. \quad (2)$$

If we assume that all IDPs start in the second QW and IDP separation increases linearly with film thickness, the average separation \bar{r} is given by

$$\bar{r} = \frac{1}{10} \sum_{i=1}^{10} r_i = \frac{9}{10} (r_2 + 8d \tan \theta), \quad (3)$$

where r_i is the separation of IDP in i th QW, d is the superlattice period, and θ is the inclination angle. With $r_2 = 20$ nm, $d = 23$ nm, $\theta = 20^\circ$, and $N = 1/\epsilon = 91$, we find $\bar{r} = 78$ nm and through Eq. (2), $\overline{\Delta\epsilon} = 3.4\%$. This is in good agreement with the results of the x-ray reciprocal space mapping, supporting our model's assumptions.

V. OPTICAL PERFORMANCE

In electro-optical characterization, the light output power of the LED on bulk GaN (sample A) is around 3.8 mW at a current of 20 mA (density of 2.5 A/cm²), as collected from the backside of the wafer. This is 25% higher than in the LED (sample C) on sapphire at similar wavelength. On the other hand, the density of inclined dislocations (6×10^9 cm⁻²) is ten times higher than that of vertical threading dislocations (typically 5×10^8 cm⁻²) in sample C or other typical LEDs on sapphire. Apparently, the light out-

put performance of green LEDs is less sensitive to edge-type inclined dislocations than to vertical threading dislocations.

VI. CONCLUSIONS

In summary, pairs of inclined dislocations were observed in the active region of green LEDs homoepitaxially grown on low-dislocation density bulk GaN. The two dislocations within one IDP start within some 20 nm in the same QW and then tilt by $18^\circ - 23^\circ$ from $[0001]$ toward different $\langle 1\bar{1}00 \rangle$ directions, usually separated by either 120° or 180° . The averaged GaInN/GaN MQW layers show some 5% of biaxial strain relaxation. We propose a model which quantitatively explains the findings by the stepwise removal of lattice points between the separating dislocations lined up along opposing $\langle 1\bar{1}00 \rangle$ directions. A quantitative microscopic analysis of the force components acting on the dislocations failed to describe the observed dislocation climb. A new macroscopic model of the strain relaxation provides a good quantitative agreement with experiment. In spite of a high density of IDPs, the green LED on bulk GaN shows a higher light output performance than its counterpart on sapphire.

ACKNOWLEDGMENTS

This work was supported by a DOE/NETL Solid-State Lighting Contract of Directed Research under Grant No. DE-FC26-06NT42860 (Brian Dotson).

*Present address: SRI International, Largo, FL, USA.

- ¹I. Akasaki, in *Nitride Semiconductors*, edited by F. A. Ponce *et al.*, MRS Symposia Proceedings No. 482 (Materials Research Society, Pittsburgh, 1998), p. 1.
- ²T. Mukai, M. Yamada, and S. Nakamura, Jpn. J. Appl. Phys., Part 1 **38**, 3976 (1999).
- ³C. Wetzel, T. Salagaj, T. Detchprohm, P. Li, and J. S. Nelson, Appl. Phys. Lett. **85**, 866 (2004).
- ⁴B. Jähnen, M. Albrecht, W. Dorsch, S. Christiansen, H. P. Strunk, D. Hanser, and Robert F. Davis, MRS Internet J. Nitride Semicond. Res. **3**, 39 (1998).
- ⁵H. K. Cho, J. Y. Lee, C. S. Kim, and G. M. Yang, J. Electron. Mater. **30**, 1348 (2001).
- ⁶X. H. Wu, C. R. Elsass, A. Abare, M. Mack, S. Keller, P. M. Petroff, S. P. DenBaars, J. S. Speck, and S. J. Rosner, Appl. Phys. Lett. **72**, 692 (1998).
- ⁷Y. Chen, T. Takeuchi, H. Amino, I. Akasaki, N. Yamada, Y. Kaneko, and S. Y. Wang, Appl. Phys. Lett. **72**, 710 (1998).
- ⁸M. Zhu, T. Detchprohm, S. You, Y. Wang, Y. Xia, W. Zhao, Y. Li, J. Senawiratne, Z. Zhang, and C. Wetzel, Phys. Status Solidi C **5**, 1777 (2008).
- ⁹D. Hanser, M. Tutor, E. Preble, M. Williams, X. Xu, D. Tsvetkov, and L. Liu, J. Cryst. Growth **305**, 372 (2007).
- ¹⁰J. Weertman, *Dislocation Based Fracture Mechanics* (World Scientific, Singapore, 1996).
- ¹¹T. Detchprohm, M. Zhu, Y. Xia, Y. Li, W. Zhao, J. Senawiratne, and C. Wetzel, Phys. Status Solidi C **5**, 2207 (2008).

- ¹²S. Nakamura, M. Senoh, N. Iwasa, S. Nagahama, T. Yamada, and T. Mukai, Jpn. J. Appl. Phys., Part 2 **34**, L1332 (1995).
- ¹³A. J. Ptak, L. Wang, N. C. Giles, T. H. Myers, L. T. Romano, C. Tian, R. A. Hockett, S. Mitha, and P. Van Lierde, Appl. Phys. Lett. **79**, 4524 (2001).
- ¹⁴M. Hawkrige, D. Cherns, and T. Myers, Appl. Phys. Lett. **89**, 251915 (2006).
- ¹⁵P. Cantu, F. Wu, P. Waltereit, S. Keller, A. E. Romanov, U. K. Mishra, S. P. DenBaars, and J. S. Speck, Appl. Phys. Lett. **83**, 674 (2003).
- ¹⁶D. M. Follstaedt, S. R. Lee, P. P. Provencio, A. A. Allerman, J. A. Floro, and M. H. Crawford, Appl. Phys. Lett. **87**, 121112 (2005).
- ¹⁷A. E. Romanov and J. S. Speck, Appl. Phys. Lett. **83**, 2569 (2003).
- ¹⁸D. M. Follstaedt, S. R. Lee, A. A. Allerman, and J. A. Floro, J. Appl. Phys. **105**, 083507 (2009).
- ¹⁹G. P. Dimitrakopoulos, Ph. Komninou, Th. Kehagias, S. L. Sakhonta, J. Kioseoglou, N. Vouroutzis, I. Hausler, W. Neumann, E. Iliopoulos, A. Georgakilas, and Th. Karakostas, Phys. Status Solidi A **205**, 2569 (2008).
- ²⁰S. Srinivasan, L. Geng, R. Liu, F. A. Ponce, Y. Narukawa, and S. Tanaka, Appl. Phys. Lett. **83**, 5187 (2003).
- ²¹R. Liu, J. Mei, S. Srinivasan, H. Omiya, F. A. Ponce, D. Cherns, Y. Narukawa, and T. Mukai, Jpn. J. Appl. Phys., Part 2 **45**, L549 (2006).
- ²²Y. Xin, S. J. Pennycook, N. D. Browning, P. D. Nellist, S. Si-

- vananthan, F. Omnès, B. Beaumont, J. P. Faurie, and P. Gibart, Appl. Phys. Lett. **72**, 2680 (1998).
- ²³A. Kelly, G. W. Groves, and P. Kidd, *Crystallography and Crystal Defects*, rev. ed. (Wiley, New York, 2000).
- ²⁴A. F. Wright, J. Appl. Phys. **82**, 2833 (1997).
- ²⁵J. W. Matthews and A. E. Blakeslee, J. Cryst. Growth **27**, 118 (1974).
- ²⁶D. Chidambarrao, G. R. Srinivasan, B. Cunningham, and C. S. Murthy, Appl. Phys. Lett. **57**, 1001 (1990).
- ²⁷A third Burgers vector may be needed to complete the Burgers circuit in 120° arrangement.
- ²⁸D. J. Bottomley and F. Fons, Jpn. J. Appl. Phys., Part 2 **34**, L1616 (1995).